Using super-stacking and super-resolution properties of time-reversal mirrors to locate trapped miners

Sherif M. Hanafy, Cairo University
Weiping Cao, Kim McCarter, and Gerard T. Schuster, University of Utah

Deadly mine collapses have recently occurred in West Virginia (January 2007, two miners killed); Russia (March 2007, 106 miners killed); Utah (August 2007, six miners and another three from the rescue team killed); Colombia (October 2007, 24 miners killed); and many other places. Locating trapped miners as soon as the collapse occurs will save lives and avoid dangerous searches in the wrong places.

Over the last two decades, many methods have been proposed for finding trapped miners. One such method is the echo location technique, where seismic emissions from a trapped miner are recorded by surface geophones, and direct arrival times are picked and used to triangulate to the miners. Unfortunately, such a method has not proven reliable, partly because the signal-to-noise ratio (SNR) of the miner's vibrations is too weak for conventional imaging methods. To partly overcome this problem, we propose applying the principle of time-reversal mirrors (TRM) to seismic data to locate trapped miners. The key idea is to estimate calibration records by using hammer sources at predetermined locations (labeled as communication stations) inside the mine and recording the seismograms with receivers on the Earth's surface. These calibration records will be used as input to a TRM to identify the location of the trapped miners. The calibration records partly overcome the poor SNR and limited aperture problems by stacking all transmitted scattered and reflected events in the data.

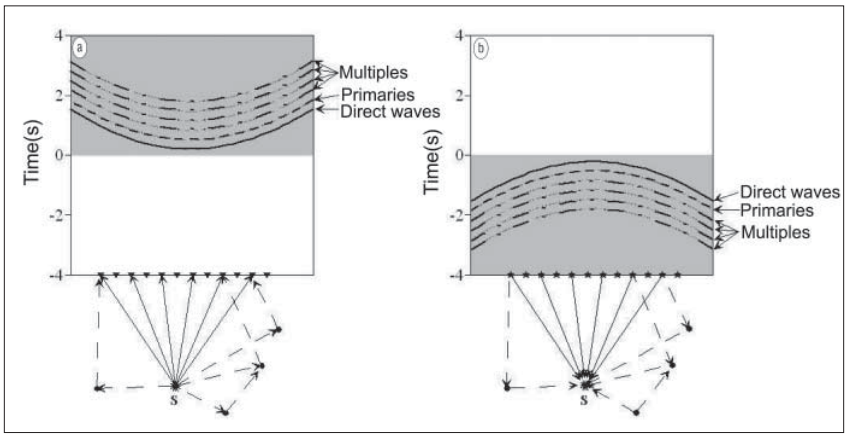

Figure 1. *(a) Forward modeled and (b) backward modeled seismic events for a source exploded at S and surface seismic recording at N geophones; solid circles indicate scatterers. Imaging of the multiple scattering events allows us to surpass the Rayleigh resolution law (i.e., super-resolution) and the law of noise suppression (i.e., super-stacking).*

Two field tests are made to test the feasibility of TRM in the noise environment; the first is a seismic experiment over a steam-pipe tunnel at the University of Utah, and the second is an experiment at a mine in Tucson, Arizona. Results at both sites show that TRM can sometimes locate trapped miners, even with SNR as low as 0.0005. Tests also validated both the super-resolution and the super-stacking properties of TRM.

Theory

Gajewski and Tessmer (2005) presented a seismic migration method to image unknown source locations with hidden excitation times. This imaging method is equivalent to standard poststack migration, except trial time shifts are introduced into seismic records to compensate for the unknown excitation time of the source. The migration images are compared for different time shifts, and the localized maxima of migration amplitudes pinpoints the unknown source locations.

The migration image $m(\mathbf{x},t)$ is given by

$$m(\mathbf{x},t) = \sum_{g} d(\mathbf{g}, \tau_{xg} + t|\mathbf{s}, t_{source}) \qquad (1)$$

where $d(\mathbf{g},\tau_{xg}+t|\mathbf{s}, t_{source})$ represents the time-differentiated passive data recorded at time $\tau = \tau_{xg}+t$ and at location $\mathbf{g}$ for a source at $\mathbf{s}$ with unknown excitation time t_{source}; and τ_{xg} is the traveltime from $\mathbf{x}$ to $\mathbf{g}$ computed by tracing rays in an assumed velocity model. Here, the variable t is the trial time shift to compensate for a nonzero excitation time, and $\mathbf{x}$ is the trial image point. Choosing the trial time $t \rightarrow t_{source}$ and trial source location $\mathbf{x} \rightarrow \mathbf{s}$ yields the maximum migration image at the actual source location $\mathbf{s}$.

A problem with this approach is that passive data are often very noisy so that a migration image contains an ambiguous maximum, leading to poor resolution of the source location. Another problem is that the velocity model must be known in order to accurately compute τ_{xg} by ray tracing. To overcome these problems, we propose to migrate the passive data with recorded calibration signals, i.e.,

$$m(\mathbf{x},t) = \sum_{g} d(\mathbf{g}, t|\mathbf{s}, t_{source}) * g(\mathbf{x},-t|\mathbf{g}, 0) \qquad (2)$$

where $g(\mathbf{x},t|\mathbf{g},0)$ is the recorded calibration record of the Earth and the convolution denoted by $*$ is over the time variable t. This calibration record is recorded and accounts for the direct wave but also contains all primaries and multiples. Equation 2 can be interpreted as the crosscorrelation of any shot gather with the calibration record.

Figure 1 illustrates the super-stacking feature of interferometric imaging where a buried source at $\mathbf{s}$ excites the scattered events seen in Figure 1a. Direct waves, primary reflections, and multiples are recorded along the surface. Back projecting these events is equivalent to replacing the geophones at the surface by loudspeakers, activating these loudspeakers after reversing the recorded time history, and using reversed traces as source time histories of the loudspeakers; in other words it

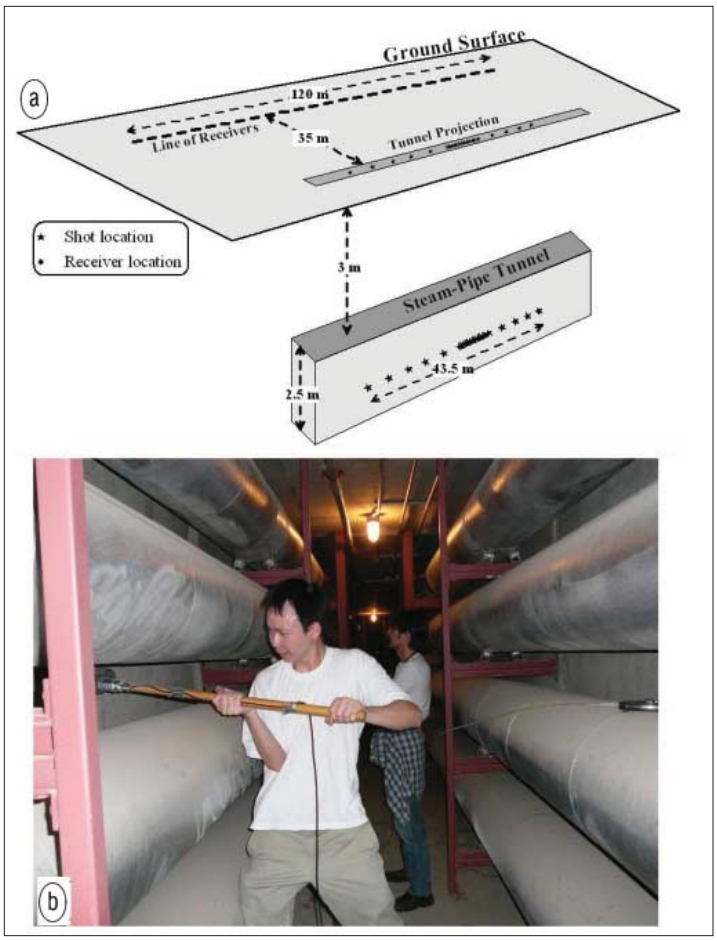

Figure 2. *(a) Sketch showing the source and receiver lines for the University of Utah field test in the steam-pipe tunnel. (b) Photo shows Chaiwoot Boonyasiriwat with the hammer source inside the steam tunnel at the University of Utah.*

is equivalent to making the surface act as a time reverse mirror. As shown in Figure 1b, backward modeling coherently returns the recorded events to their common source point at the excitation time of $t = 0$. The estimated migration amplitude is a maximum at the source point location **s** because all backprojected direct waves, primaries, and multiples are simultaneously in phase at the source excitation time ($t = 0$ in this example).

This procedure is equivalent to time-reverse acoustics, where multiple scattering events can be used for super-resolution imaging, and provide a super-stack capability by using all direct, primary and multiple scattering events for focusing. For additive white noise, this means that the SNR of the data is enhanced by a factor of $\sqrt{\frac{T}{T_o}N}$ where T is the total recorded time/shot, T_o is the wavelet period, and N is the number of traces. This assumes that all events in the record are of similar amplitude and there are $\frac{T}{T_o}$ recorded events in each trace. In comparison, the standard migration equation only sums the N traces along the direct wave hyperbola for a SNR enhancement factor of $\sqrt{N}$.

Spatial resolution is defined as the ability to separate two features that are very close together, i.e., the minimum separation of two bodies before their individual identities are lost. The distance between the two features must be, roughly, greater than or equal to ½ of the dominant wavelength λ. More precisely, the Rayleigh resolution limit Δx for imaging zero-offset seismic data is given as

$$\Delta x = \frac{\lambda z}{2L} \tag{3}$$

where L is the length of the receiver line, and z is the depth of the point source.

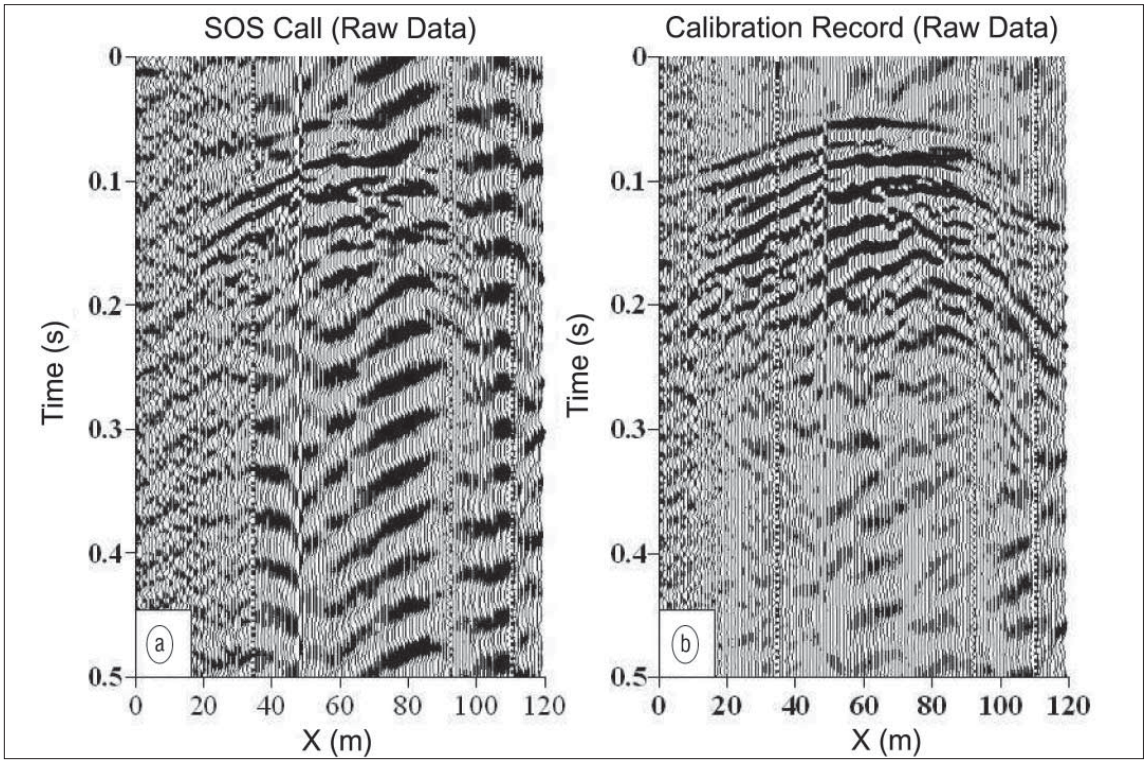

Figure 3. *SOS and calibration record examples for the steam tunnel test. (a) Raw SOS shot gather. (b) A calibration record (raw data). The SOS and calibration record shot gathers are obtained from shot number 5 (at X = 16 m).*

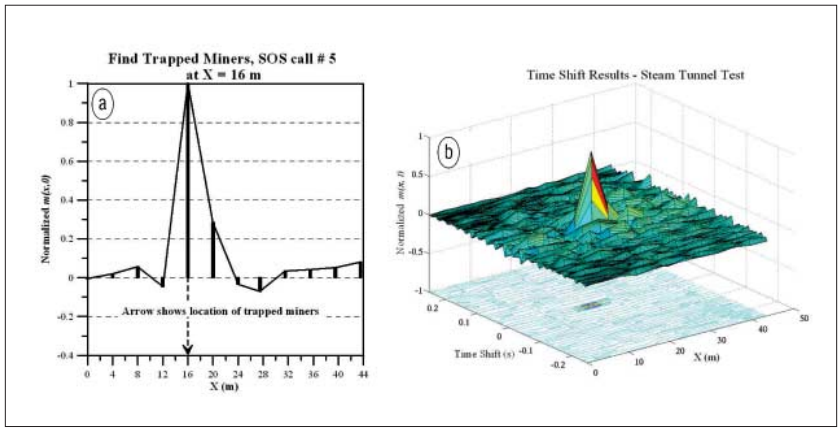

Figure 4. *(a) A graph of m(x,0) versus* x *computed for the steam-tunnel data, where the SOS location is at* x = *16 m, which coincides with the maximum value of the curve. (b) The migration image m(x,t) computed for the steam-tunnel data. The peak corresponds to the actual SOS source location in the steam tunnel and the correct excitation time.*

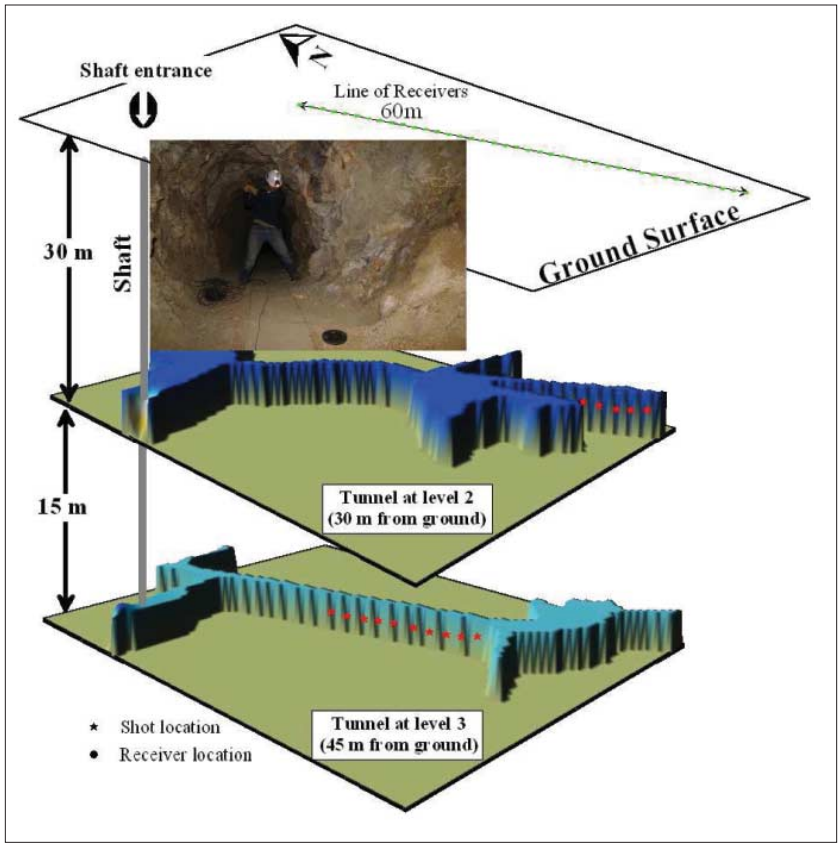

Figure 5. *Sketch showing the different mine levels, source locations, and receiver lines for data collected at the Tucson site. The small photo shows Naoshi Aoki hammering inside the San Xavier mine.*

To overcome the restricted limitation of the Rayleigh resolution limit, TRM focus all scattered waves, instead of focusing only the direct waves, with a quasi-uniform distribution of incidence angles. In this work we applied TRM to seismic data to demonstrate that it can detect the location of trapped miners in a low signal-to-noise environment. These data were also used to demonstrate the super-resolution and the super-stacking capability of TRM. TRM is equivalent to reverse-time migration with an exact velocity model, except the velocity model is not needed.

Field tests

Two sets of data were collected to test the TRM approach. A Bison 24000 with 120 channels is used to record the data with a sledge hammer (16 lbs) used as the seismic source.

University of Utah steam-tunnel test. This set of data was recorded on the University of Utah campus. A hammer is used to strike the wall of an underground steam-pipe tunnel (Figure 2a). The tunnel is approximately 300 m long, 2 m high, 2.5 m wide, and about 3 m below the surface. Twenty-five "shots" (Figure 2b) were used with the following spatial offset intervals: shots 1–6 and 20–25 have a shot interval of 4 m; shots 6–20 have denser intervals of 0.5 m. The denser shot distribution was used to test the super-resolution property of TRM. The recording array consists of 120 receivers with a receiver interval of 1 m. The receiver line is on the surface 35 m from the tunnel (Figure 2a). At each shot location, two files were recorded: (1) a one-stack CSG that represents the recorded vibrations from the miners (Figure 3a) which we call the SOS data and (2) the calibration record obtained by stacking 20 shot gathers (Figure 3b). Two processing steps prepared the data for interpretation: a 5–100 Hz band-pass filter to remove high-frequency noise, and trace normalization of each CSG (amplitude values of each trace are divided by the maximum absolute amplitude value of that trace).

Applying the TRM approach to the SOS signal—$d(\mathbf{g},t|\mathbf{s},0)$ in Equation 2—yields the graph in Figure 4a. Repeating the process for all SOS shot gathers gives the correct locations of the miners and establishes that finding the trapped miners using TRM was successful for all 25 SOS locations.

A more realistic scenario is that the initiation time of the recorded SOS data source is unknown, so a time shift was applied to the recorded data. These shifted data were migrated using Equation 2. The plot of $m(\mathbf{x},t)$ in Figure 4b shows the maximum value at the correct source location and excitation time.

Tucson test. The data were collected at the San Xavier experimental site south of Tucson which contains three mine levels. The "shots" were fired in the second and third tunnels (30 and 45 m below the ground) with the receivers on the surface (Figure 5). The receiver line consisted of 120 receivers

with a separation of 0.5 m. Twenty-five hammer stations were placed at 0.5 m and 0.75 m intervals in the second and third levels, respectively. For each shot, two files were recorded; one represents the miner's SOS call with a one-stack shot gather (Figure 6a) and the other represents the calibration record with 16 and 22 stacks for the second and third levels, respectively (Figure 6b). We used two processing steps: a 100–160 Hz low-pass filter and trace normalization were applied to each shot gather (the normalization factor for each trace is the maximum absolute value of that trace).

Figure 7a shows that applying Equation 2 to these data identifies the exact location of the SOS shot points. These results are similar to the steam-tunnel results in the sense that the time-shift test identifies the correct SOS location as well as its excitation time (Figure 7b).

Super-stack test. In an actual mine emergency, we do not expect the SOS call to have high or even a good SNR. To show that TRM can overcome a low SNR, a super-stacking test was applied to both data sets. Random noise was generated and then filtered using the same band-pass parameters used to filter the recorded data. The resulting filtered random noise was added to the recorded SOS calls (Figures 8a and 8b). The final result is then correlated with the 25 calibration records. Here, the SNR of the SOS data are 1/1738 for the steam-tunnel test and 1/2670 for the Tucson tests. The resulting images (Figures 8c and 8d) show that the location of the trapped miners can still be identified.

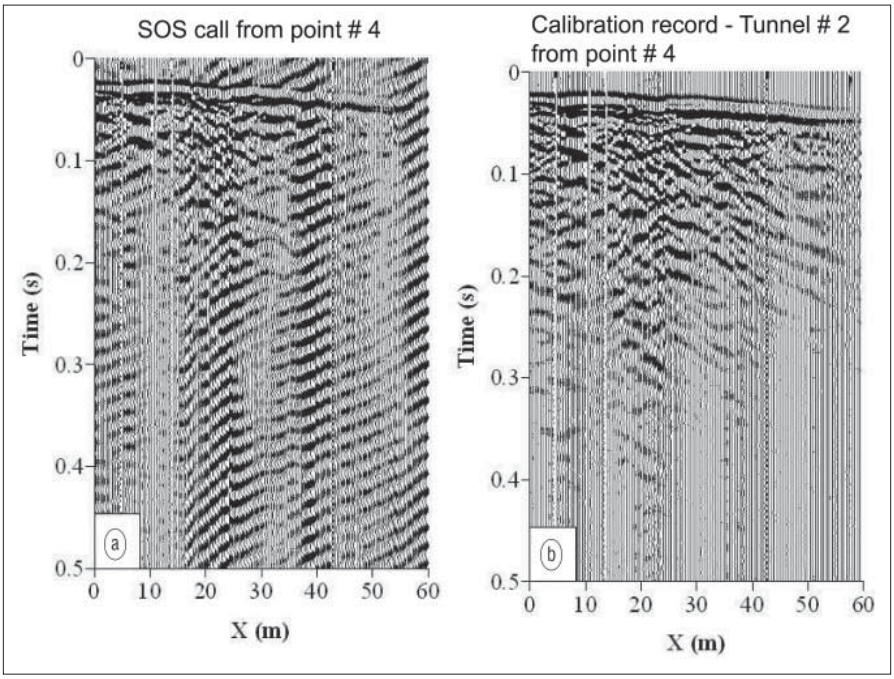

Figure 6. *Two shot gathers from the Tucson data set: (a) SOS record from tunnel 2. (b) calibration record from tunnel 2.*

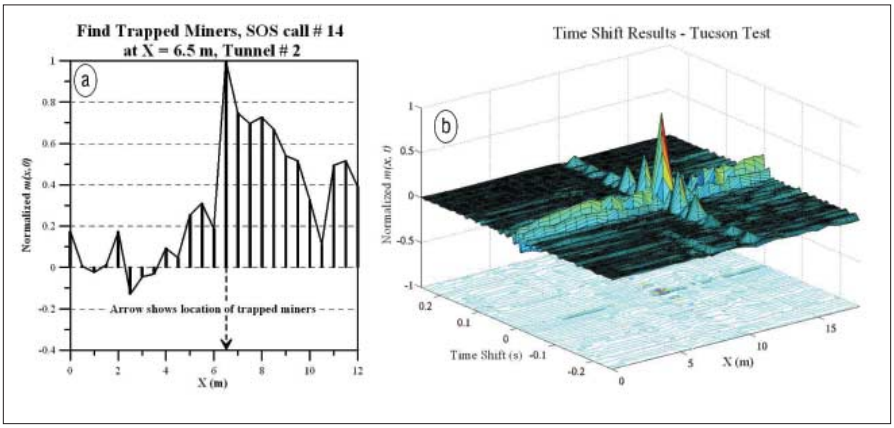

Figure 7. *(a) An example shows m(x, 0) versus* x *computed for Tucson data (tunnel 2), the actual SOS call location is at* x = *6.5 m, which coincides with the maximum value of the curves. (b) Migration image m(x,t) for result from tunnel 3, it shows a maximum peak at the correct SOS locations and correct zero times.*

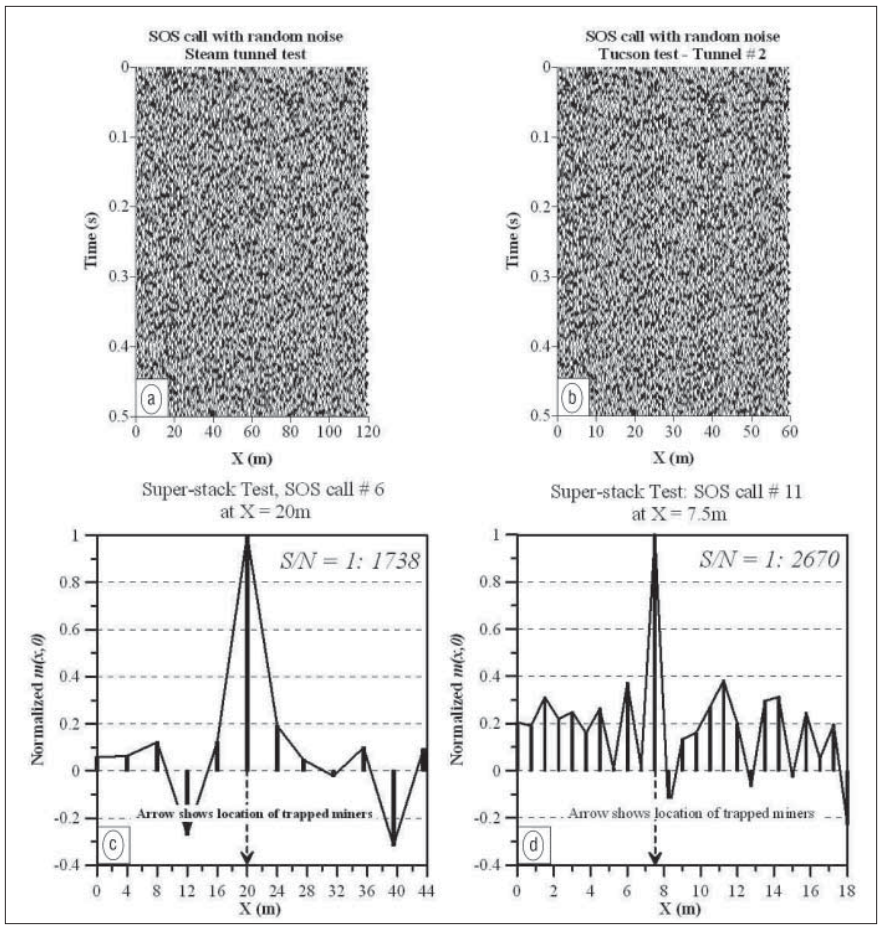

Figure 8. *Two examples show SOS call after adding random noise to decrease the S/N ratio. (a) SOS reecord from steam tunnel data set with S/N = 1:1738. (b) SOS record from Tucson data set, tunnel 3 with S/N = 1:2670. (c) The results after using the low S/N data as input into the TRM algorithm for the steam tunnel test, and (d) for the Tucson tunnel 3 data set. Compare (c) with Figure (4a) and (d) with Figure (7a).*

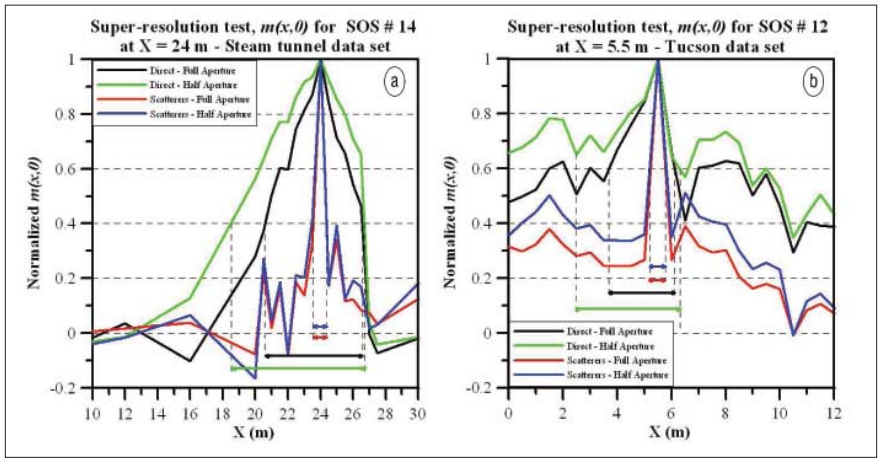

Figure 9. *The super resolution results from the (a) steam tunnel field test and the (b) Tucson field test—tunnel 2. Both results suggest that the Rayleigh resolution limit can be reduced by a factor of 3 or more if all scattered events are used for focusing. The horizontal resolution limit is taken to be the width of main lobe at the amplitude that is 50% of the peak amplitude value.*

Super-resolution test. The super-resolution property was evaluated for both the steam-tunnel and Tucson-data sets. The collected shot gathers are separated into (1) a scattered shot gather (only scattered energy is present after removing the direct waves) and (2) a direct-wave shot gather (only direct-wave energy is present). Selected SOS scattered-only shot gathers are correlated with all scattered-only calibration records, and selected SOS direct-only shot gathers are correlated with all direct-only calibration records. The results obtained using the full 120-trace aperture width are compared to those for a half-aperture width of 60 traces. Figures 9a and 9b show the plot of $m(\mathbf{x},0)$ computed from both the steam tunnel and Tucson data. Each plot contains 4 curves: (1) correlation results $m^{dir}(\mathbf{x},0)$ from traces that contain only direct waves using the full aperture width (120 m and 60 m at Utah and Tucson data sets, respectively); (2) Correlation results $m^{\frac{dir}{2}}(\mathbf{x},0)$ from traces that contain only direct waves using a half-aperture width (60 and 30 m, respectively); (3) correlation results $m^{scatt}(\mathbf{x},0)$ from traces that contain only scattered data using the full aperture width; (4) correlation results $m^{\frac{scatt}{2}}(\mathbf{x},0)$ from traces that contain only scattered data using a half aperture width.

If the spatial resolution limit is defined as the width of the main lobes (see arrows in Figures 9a and 9b), the images show:

- Spatial resolution limits of $m^{scatt}(\mathbf{x},0)$ and $m^{\frac{scatt}{2}}(\mathbf{x},0)$ are much smaller than for $m^{dir}(\mathbf{x},0)$ and $m^{\frac{dir}{2}}(\mathbf{x},0)$.
- If only direct arrivals are used, the minimum resolution width increases as the aperture is decreased.
- If only scattered arrivals are used, aperture width does not affect the spatial resolution.

The results using only scattered waves show spatial resolution limits 5–7 times better than using only direct-wave arrivals and independent of the aperture width, which is 5–7 times better than the Rayleigh resolution limit.

Conclusions

We have described a TRM method to locate miners trapped in a collapsed mine. This approach consists of two stages. First, use surface receivers that overlie the mine to record calibration records for sources at predetermined communication stations inside the mine tunnels. When a collapse occurs, the trapped miners should find the nearest communication station inside the mine and send a

SOS call using a small hammer. Recording this SOS call with the fixed receiver line and cross correlating, the SOS data with the calibration records can identify the location of the trapped miners. Calibration records may vary due to mining activity, so they should be updated periodically.

There are several possible problems with this approach, among them the zero time of the SOS is unknown, and the SOS call is expected to have very low SNR. The TRM approach mitigates both problems by time shifting the input data to identify the miners' location and the initiation time of the SOS call. Random noise added to the SOS calls and experimental results show that, even with the very low SNR, the location of the trapped miner can be determined.

The implication is that a coded message can be sent by the miner. Two-way communication can be made if a geophone is at the communication station and surface sources are excited, data are recorded, and the time delays are applied to these data so they focus the wavefield to the communication station.

An important result here is that we demonstrated that the Rayleigh resolution limit can be exceeded if the multipath events are used in conjunction with TRM. To our knowledge, this is the first field experimental verification of the TRM super-resolution property with a realistic seismic experiment. We also believe that this is the first time that the super-stack property is recognized and validated with field data.

Suggested reading. "Reverse modeling for seismic event characterization" by Gajewski and Tessmer (*Geophysical Journal International*, 1996). "Time-reversed acoustics" by Fink (*Physics Today*, 1997). "Communication through a diffusive medium: coherence and capacity" by Moustakas et al. (*Science*, 2000). "Overcoming the diffraction limit in wave physics using a time-reversal mirror and a novel acoustic sink" by de Rosny and Fink (*Physical Review Letters*, 2002). TLE

Acknowledgments: We thank the American Chemical Society and the 2007 sponsors of the University of Utah Tomography and Model/Migration (UTAM) Consortium for their support. We thank N. Aoki, C. Boonyasiriwat, S. Dong, S. Liu, G. Zhan, X. Xiao, and Y. Xue for helping with data acquisition. Finally, we thank Ross Hill, director of the San Xavier Laboratory, for his help during data acquisition.

Corresponding author: sherif.geo@gmail.com